Growing Process of Scattering Density Fluctuation of a Medium Distance in the Hydrogel of Poly(vinyl alcohol) under Stretching

Mitsuhiro Hirai,*,† Toshihiro Hirai,‡ and Tatsuo Ueki§

Faculty of General Studies, Gunma University, 4-2 Aramaki, Maebashi-shi 371, Japan, Faculty of Textile Science and Technology, Shinshu University, 3-15-1 Tokida, Ueda-shi 386, Japan, and The Institute of Physical and Chemical Research, 2-1 Hirosawa, Wako-shi 351-01, Japan

Received July 19, 1993; Revised Manuscript Received November 1, 1993®

ABSTRACT: The small-angle X-ray scattering technique using synchrotron radiation was employed to study the conformational change of the hydrogel of poly(vinyl alcohol) (PVA) under stretching. In the stretching process the PVA molecule in the gel mostly retains a folded structure as a structural domain characterized by a fractally rough interface which slightly changes. Simultaneously, the stretching not only induces the long-range orientation of the domains in the gel but also enhances a scattering density fluctuation with the medium distance of about 20 Å, accompanying the short-range ordering known to be microcrystallization. Alternatively, in the case of the PVA hydrogel the stretching gradually induces the rearrangement of the polymer chains around cross-linking points in the domain, which exhibits the scattering density fluctuation with about a 20-Å length scale, resulting in the microcrystallization over the gel to show the diffraction peak of crystallites in the high q region.

I. Introduction

We have found that the hydrogel of poly(vinyl alcohol) (PVA) can possess remarkable shape memorizing properties.[1-3] In the properties, strains induced by stretching are shown to be fixed stable and lead to the shape memory.

The effect of stretching on the gel structure together with its physical properties has been investigated by other authors.[4-10] On the process of gel elongation up to 400%, they observed the change of diffraction pattern at the high q region from 1.4 to 2.5 Å^{-1} (where $q = 4\pi (\sin \theta)/\lambda$, 2θ = scattering angle, λ = wavelength used), concluding that the elongation led the orientation of the polymer chain and intensified the diffraction peak at $q = 1.382$ Å^{-1} by the increase of the crystallite of PVA.[9] The strain fixing to the gel and its effect on the contraction process have been investigated by the authors.[11] We observed the similar effect of the strain fixing process on the X-ray diffraction pattern at the same q region as mentioned above and clarified that the contraction process becomes asymmetric by the anisotropy of the gel network.

In the present study, we have focused on clarifying the structural change of the PVA gel under stretching at small and medium scattering angle regions. This report will show the new evidence of the effect of stretching on the structural change of the gel network by using the small-angle X-ray scattering method.

II. Experimental Section

1. Sample Preparation. The PVA used was Kralay 117 (DP = 1700) after purification by conventional methods as follows. First, the PVA was completely hydrolyzed with NaOH, repetitively precipitated by pouring aqueous solution of the PVA into acetone, and then completely dried in vacuo. A 10% aqueous solution (w/w) of the purified PVA was cast in a Petri dish and served for repetitive freezing and thawing for six times. The freezing and thawing processes were carried out for 23 h at −20 °C and for 1 h at room temperature, respectively. Then the prepared hydrogel was immersed in water until ready for measurements.

2. Small-Angle X-ray Scattering Experiments. Small-angle X-ray scattering measurements were performed by using the synchrotron radiation X-ray scattering spectrometer for enzymes, which is installed in the Photon Factory of the National Laboratory for High Energy Physics, Tsukuba, Japan. The incident X-ray beam intensity was monitored using an ionization chamber placed in front of samples, and the scattering data were collected using a one-dimensional position sensitive proportional counter (PSPC) with a probe 20 cm in effective length. The details of the instruments were explained elsewhere.[12] The measurements were carried out at room temperature on the following conditions: wavelength, 1.49 Å; sample-to-detector distance, 87 cm; exposure time, 60 s. The sample holder designed for gel stretching experiments was used. The dimensions of the PVA gel sheet used were 15.7 × 1 mm in cross section and 45 mm in length. The gel sheet was stretched by using variable weights in the range from 0 to 300 g. The direction of elongation of PVA gel was perpendicular to that of the PSPC anode. The measured scattering intensity was corrected by the transmission deduced from the elongation degree of the sample and by the subtraction of background scattering.

3. Analysis of Scattering Profiles. After the above correction of the scattering data, the following analyses were carried out. The Guinier analysis was done for the beginning of the scattering curve by using the Guinier equation in the form

$$I(q) = I(0) \exp(-q^2 R_g^2/3) \tag{1}$$

where q is the magnitude of the scattering vector, R_g is the radius of gyration, and $I(0)$ is the zero-angle scattering intensity.[13] We tentatively chose the scattering data in the q range 0.02–0.03 Å^{-1} and determined the apparent value of the radius of gyration R_g* by using the least-squares method for the Guinier plot (ln $I(q)$ versus q^2) on the data sets in this q range.

For the middle scattering angle region which is larger than the particle size ($qR_g \gg 1$) but smaller compared to typical chemical bond distances a ($qa \ll 1$), it is known that the scattering curves depend on the simple power law given by

$$\log I(q) = \text{const} + \alpha \log q \tag{2}$$

where α is the Porod slope. As is well-known, the evaluation of the Porod slope is useful in characterizing and ascertaining the geometric properties of random structures.[14-24]

The analysis using the distance distribution function $p(r)$ was done by calculating the Fourier inversion of the scattering intensity $I(q)$ as

$$p(r) = \frac{2}{\pi}\int_0^\infty rqI(q) \sin(rq)\, dq \tag{3}$$

It depends both on the particle geometry, expressing numerically

† Gunma University.
‡ Shinshu University.
§ The Institute of Physical and Chemical Research.
® Abstract published in *Advance ACS Abstracts,* January 15, 1994.

0024-9297/94/2227-1003$04.50/0 © 1994 American Chemical Society

the set of distances joining the volume elements within the particle, and on the inner scattering density distribution in the particle. To calculate the function $p(r)$, the extrapolation method was done by using the least-squares method on the Guinier plot for the small-angle data sets, and the modified intensity as

$$I'(q) = I(q) \exp(-kq^2) \quad (4)$$

(k is the artificial damping factor) was used to remove the Fourier truncation effect. The maximum diameter $D_{max}(r)$ of the particle was determined by the $p(r)$ function satisfying the condition $p(r) = 0$ for $r \geq D_{max}$. The total scattering power I_{total} is obtained by

$$I_{total} = \int_0^{D_{max}} p(r)\, dr \quad (5)$$

which was used for normalization of the $p(r)$ function.

4. Modeling Analysis. According to the convolution theory the structural factor $A(\mathbf{q})$ of a particle composed of several shells with difference average scattering densities can be described generally as follows:

$$A(\mathbf{q}) = \bar{\rho}_1 \int_{v_1} \rho_1(\mathbf{r}) \exp(i\mathbf{q}\cdot\mathbf{r})\, d\mathbf{r} + \sum_{i=2}^{n} (\bar{\rho}_i - \bar{\rho}_{i-1}) \int_{v_i} \rho_i(\mathbf{r}) \exp(i\mathbf{q}\cdot\mathbf{r})\, d\mathbf{r} \quad (6)$$

where $\bar{\rho}_i$ is the average scattering density and of ith shell with a shape function $\rho_i(\mathbf{r})$. Therefore the scattering intensity for an ellipsoid of rotation composed of shells is given as

$$I(q) = \langle A(\mathbf{q})A^*(\mathbf{q}) \rangle = \int_0^1 \left[3\sqrt{\frac{\pi}{2}} \{ \bar{\rho}_1 V_1 J_{3/2}(qR_1)/(qR_1)^{3/2} + \sum_{i=2}^{n} (\bar{\rho}_i - \bar{\rho}_{i-1}) V_i J_{3/2}(qR_i)/(qR_i)^{3/2} \} \right]^2 dx \quad (7)$$

where $\langle\,\rangle$ means the spherical average of the scattering intensity $I(\mathbf{q})$ defined as $A(\mathbf{q})A^*(\mathbf{q})$, $J_{3/2}$ is the 3/2th Bessel function, and R_i is defined as

$$R_i = r_i(1 + x^2(\nu_i^2 - 1))^{1/2} \quad (8)$$

where r_i and ν_i are the semiaxis and its ratio of the ith ellipsoidal shell, respectively. By using eqs 3 and 7, we can simulate the distance distribution function for an ellipsoid of rotation with some inner scattering density fluctuation to a certain extent.

III. Results and Discussion

Figure 1 shows the small-angle scattering profiles $I(q)$ on the stretching process where logarithms of $I(q)$ are plotted as a function of log q. The decrease of intensity below 0.015 Å^{-1} is attributed to the beam stopper. It is apparent that the scattering profile changes systematically with increasing stress. The increase of the scattering intensity in the small q region at around 0.02 Å^{-1} results from a long-range orientation of PVA molecules in the gel. At the medium q region of 0.2–0.4 Å^{-1}, as shown in the insert of Figure 1, the broad peak at around 0.3 Å^{-1} becomes gradually evident. It implies that the local conformational ordering with the period dimension $d = 2\pi/q$ of about 20 Å was induced by stretching. As in the measurable q region under the present experimental conditions we did not observe any other evident peak or hump caused by a longer ordering with the period of up to 400 Å; the appearance of the broad peak can be attributed to a scattering density fluctuation with a 20-Å length scale, in other words, a creation of subdomains with medium. On the other hand, every scattering curve has apparently two different Porod slope regions. It shows that the two classes of fractal objects can be discussed according to the slope in the Porod regions.[19,21,22] In the process of stretching the Porod slope α at the q region of 0.03–0.048 Å^{-1} varies from −1.53(±0.01) to −1.56(±0.01), and that at the q region of 0.06–0.11 Å^{-1}

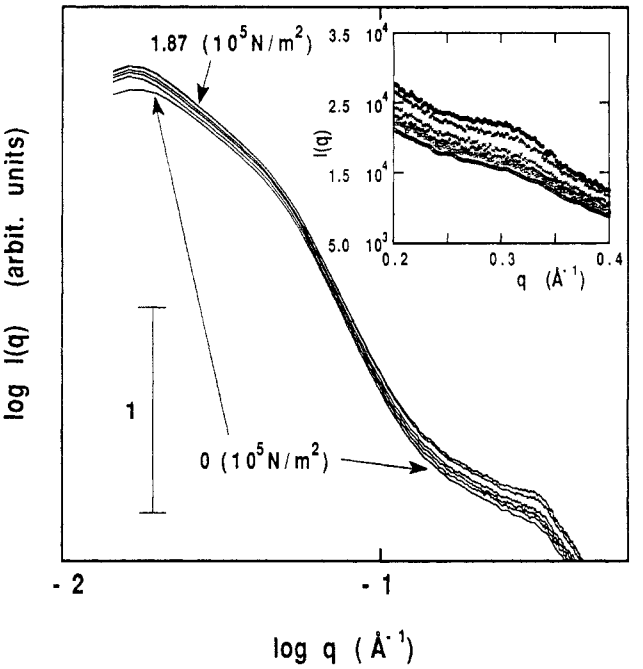

Figure 1. Change of scattering curve of the 10% PVA hydrogel (w/w) under stretching. The applied stress was varied from 0 to 1.87×10^5 N/m^2). The scattering curves are shown by the double-logarithmic scale, where the insert shows the extended profile in medium q region. The fast decrease of scattering intensity in the small q region is attributed to the beam stopper.

does from −3.197(±0.001) to −3.084(±0.001). The former and latter slopes correspond to those for volume fractals ($\alpha > -3$) and for surface ones ($-4 < \alpha < -3$), respectively. The crossover point appears at 0.05 Å^{-1}, which corresponds to a length $l = 1/q$ of 20 Å^{-1}. Then, it can be understood that the two Porod regions originate from a fractally rough surface at short length scales below 20 Å^{-1} and from a volume fractal of dimension 1.5 at larger scales; therefore, it can be assumed that the PVA gel was composed of PVA molecules as structural domains with fractally rough interfaces, and the structures of these interfaces changed gradually by stretching. The above discussion is supported by the following analyses.

To eliminate an aritifact on the Guinier analysis, we defined the q region 0.02–0.03 Å^{-1} to determine the apparent radius of gyration denoted as R_g* by using the least-squares method for the Guinier plot (ln $I(q)$ versus q^2) on the data sets of this q range. The experimental structural parameters including the R_g* values are summarized in Table 1. Although the gradual change of R_g* from 44.0(±0.9) to 45.0(±1.0) Å is comparable to the margin of experimental error, it can be assumed that the shape of the PVA molecule in the gel was mostly retained as a structural domain under stretching. This slight change is attributable to the change of the electron density distribution in the domain, as will be shown in the following paragraphs.

Figure 2a represents the distance distribution functions $p(r)$ obtained by the Fourier inversion of the experimental scattering curves in Figure 1, where each $p(r)$ function is normalized by the total scattering power evaluated using eq 5. The profiles of the $p(r)$ functions are characterized by the peaks at 47(±1) Å and the following shoulders, which shows that the structure of the PVA molecule in the gel takes a folded one as a structural domain. The maximum diameter D_{max}, namely, the maximum intraparticle vector of the domain, is approximately 179(±1) Å, which is independent of the magnitude of the applied stress under the present experimental conditions. Taking

Table 1. Characteristic Parameters of the PVA Hydrogel under Stretching (PVA concentration: 10% (w/w))

stress (10^5 N/m^2)	Porod slope[a] of 0.03–0.048 Å^{-1}	Porod slope[b] of 0.06–0.11 Å^{-1}	R_g* (Å)	D_{max} (Å)	peak position of $P(r)$ (Å)
0	−1.528 ± 0.005	−3.197 ● 0.001	44.0 ± 0.9	179 ± 1	47 ± 1
0.12	−1.529 ± 0.005	−3.173 ± 0.001	44.0 ● 0.9	180 ± 1	47 ● 1
0.31	−1.541 ± 0.005	−3.171 ± 0.001	44.3 ± 0.9	180 ● 1	47 ± 1
0.62	−1.543 ● 0.005	−3.149 ± 0.001	44.6 ± 1.0	180 ± 1	47 ± 1
1.25	−1.550 ± 0.004	−3.107 ± 0.001	44.9 ± 1.0	179 ± 1	47 ± 1
1.87	−1.556 ± 0.005	−3.084 ● 0.001	45.0 ± 1.0	179 ± 1	47 ● 1

[a,b] Poros slopes are obtained from the scattering curves at the q regions shown in the columns.

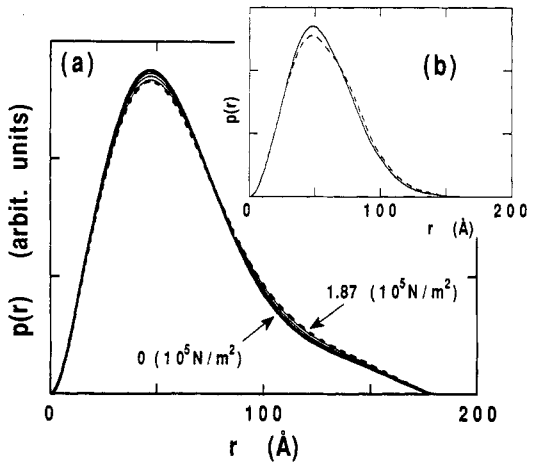

Figure 2. Distance distribution functions $p(r)$ obtained by the Fourier inversion of the experimental scattering curves (a) and of those calculated in the modeling analysis (b). Figure a: full thick line, under zero stress; dashed thick line, under maximum stress (1.87×10^5 N/m^2). Figure 2b: full line, double-shell ellipsoid (44 Å in R_g, 59.7 and 31.5 Å in the semiaxis of the outer shell and inner core, 0.31/1 ratio of scattering densities, identical semiaxial ratio of 1.5); dashed line, double-shell ellipsoid (45 Å in R_g, 63.9 and 30.0 Å in the semiaxis of the outer shell and inner core, 0.10/1 ratio of scattering densities, identical semiaxial ratio of 1.4). Those models give identical values of D_{max} and peak position as 47 and 179 Å, respectively. On the Fourier inversion the extrapolation method and the artificial damping factor were applied to the scattering curves. The $p(r)$ functions were normalized by the total scattering power estimated by using eq 5 in the text.

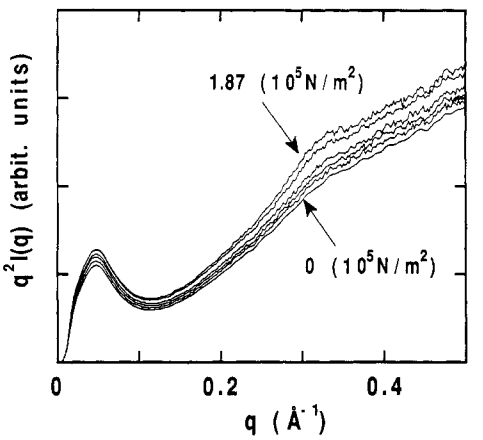

Figure 3. Kratky plots of the scattering curves in Figure 1. Peaks located at 0.046 Å^{-1}.

into account the experimental value of the radius of gyration, the D_{max} observed is much longer than the value of 121 Å for a sphere with a homogeneous electron density distribution. In addition the systematic change of the intraparticle vectors at around 50 and 120 Å induced by stretching is observed. To describe both the experimental characteristic and the change of the $p(r)$ function, we performed the simple modeling analysis using eqs 3 and 7. If we use a single hard sphere or ellipsoid having no scattering density fluctuation, the experimental profile of the $p(r)$ function can never be obtained. The minimum requirement to realize such an experimental $p(r)$ profile is to give a model structure of a double shell that may be one of the simplest models having some scattering density fluctuation. A double-shell ellipsoid with a low electron density core surrounded by a high electron density shell is not suitable because it gives an opposite $p(r)$ profile having a shoulder followed by a peak. Then the model structure of the PVA molecule is presumed to be a double-shell ellipsoid with a high electron density core surrounded by a low electron density shell. The structural parameters of the double-shell ellipsoidal models were searched to give the experimental values of D_{max} and the peak position to be 47 and 179 Å, respectively, under total scattering power. The full line in Figure 2b corresponds to the double-shell ellipsoid with 44 Å in R_g, composed of the outer shell and the inner core having respectively 59.7 and 31.5 Å in semiaxis, a 0.13/1 ratio of the scattering densities, and an identical semiaxial ratio of 1.5. The dashed line in Figure 2b corresponds to the double-shell ellipsoid with 45 Å in R_g, composed of the outer shell and the inner core having respectively 63.9 and 30.0 Å in semiaxis, a 0.10/1 ratio of the scattering densities, and an identical semiaxial ratio of 1.4. The $p(r)$ functions in Figure 2b obtained from the above modeling can describe the characteristics of the experimental $p(r)$ functions; therefore, the above systematic change of the intraparticle vector in the experimental $p(r)$ functions may be understood to result from the gradual change of the scattering density distribution in the PVA molecule by stretching.

The Kratky plots ordinarily used for persistency analysis[19,20] are given in Figure 3. Clear peaks at 0.046 Å^{-1} can be ascribed to the presence of the structural domains with folded structures compared to other parts in the gel matrix, which means that the PVA molecules mostly retain those conformations as structural domains in the gel network.

IV. Conclusions

The present results show the new evidence of the medium distance region in the conformational change of PVA gel by stretching. Under the present experimental conditions the PVA molecules in the gel mostly retained folded structures as structural domains with fractally rough interfaces. Even at low stress the stretching induced not only the long-range orientation of the PVA molecules in the gel but also the rearrangement of the polymer chains in the domains. This rearrangement caused the creation of the subdomains, resulting in the enhancement of the scattering density fluctuation with the dimension of about 20 Å. Such a feature is shown schematically in Figure 4. As PVA is known to be one of typical crystalline polymers so that the cross-linking points in the gel are believed to be crystallites, these points in the PVA gel can be expected to play an important role in the above structural change. The presence of two Porod regions suggests that the structure of the PVA hydrogel resembles that of silica aerogel.[22] The change of the Porod slope at high q region

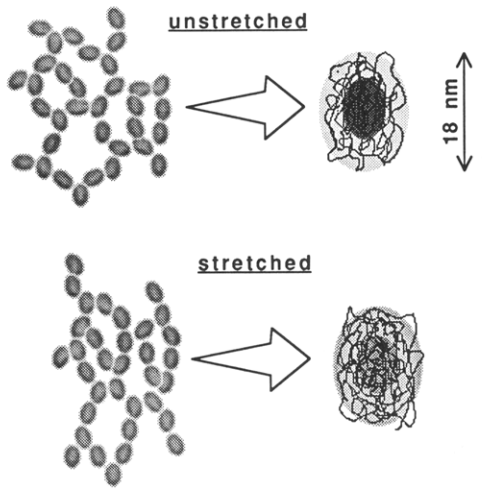

Figure 4. Schematic drawing of the structure suggested for the PVA hydrogel under stretching.

caused by stretching is attributable to the structural change of the domains at interfaces. Combined with the previous results on the high elongation process shown by other authors,[9] it can be assumed reasonably that by increasing stretching stress the gradual structural change in the domains is first induced around physically cross-linking points to create subdomains with a finite size, namely, to create the scattering density fluctuation with about a 20-Å length scale, and the microcrystallization over the gel finally becomes dominant to show the diffraction peak at a high q region, as evidence of the increase of crystallites in the gel. In other words it can be concluded that the stretching causes the rearrangements of the polymer chains around crystalline regions, followed by the enhancement of scattering density fluctuation, resulting in the crystallization over the gel.

Acknowledgment. We thank Drs. Y. Amemiya and K. Kobayashi of the Photon Factory at the National Laboratory for High Energy Physics for their help with the synchrotron radiation scattering experiments and with the maintenance of the small-angle scattering instruments. This work has been performed under the approval of the Photon Factory Program Advisory Committee (Proposal No. 92G209).

References and Notes

(1) Hirai, T. *Kobunshi (High Polymers)* **1991**, *40*, 5248.
(2) Hirai, T.; Maruyama, H.; Suzuki, T.; Hayashi, S. *J. Appl. Polym. Sci.* **1992**, *45* (7), 1849.
(3) Hirai, T.; Maruyama, H.; Suzuki, T.; Hayashi, S. *J. Appl. Polym. Sci.* **1992**, *46* (8), 1449.
(4) Watase, M.; Nishinari, K.; Nambu, M. *Polym. Commun.* **1983**, *24*, 52.
(5) Watase, M. *Nippon Kagaku Kaishi* **1983**, 973–7.
(6) Watase, M. *Nippon Kagaku Kaishi* **1983**, 1254–9.
(7) Watase, M.; Nishinari, K. *Makromol. Chem.* **1985**, *186*, 1081.
(8) Watase, M.; Nishinari, K. *Makromol. Chem.* **1988**, *189*, 871.
(9) Watase, M.; Nishinari, K. *J. Polym. Sci., Polym. Phys. Ed.* **1985**, *23*, 1803.
(10) Nishinari, K.; Watase, M.; Ogino, K.; Nambu, M. *Polym. Commun.* **1983**, *24*, 345–347.
(11) Hirai, T.; Hanaoka, K.; Suzuki, T.; Hayashi, S. *Kobunshi Ronbunshu* **1989**, *46*, 613–17.
(12) Ueki, T.; Hiragi, Y.; Kataoka, M.; Inoko, Y.; Amemiya, Y.; Izumi, Y.; Tagawa, H.; Muroga, Y. *Biophys. Chem.* **1985**, *23*, 115–124.
(13) Guinier, A. *Ann. Phys.* **1939**, *12*, 161.
(14) Porod, G. *Kolloid Z.* **1951**, *124*, 251.
(15) Daoud, M.; Joanny, J. F. I. *J. Physique* **1981**, *42*, 1359.
(16) Witten, T. A.; Sander, L. M. *Phys. Rev. Lett.* **1981**, *47*, 1400.
(17) Meakin, P. *Phys. Rev. Lett.* **1983**, *51*, 1119.
(18) Bale, H. D.; Schmidt, P. W. *Phys. Rev. Lett.* **1984**, *53*, 596.
(19) Schaefer, D. W.; Keefer, K. D.; Aubert, J. H.; Rand, P. B. In *Science of Ceramic Chemical Processin*; Hench, L. L., Ulrich, D. R., Eds.; John Wiley & Sons Inc.: New York, 1986; p 140.
(20) Shaefer, D. W.; Martin, J. E. *Phys. Rev. Lett.* **1984**, *52*, 2371.
(21) Schaefer, D. W.; Keefer, K. D. *Phys. Rev. Lett.* **1986**, *56*, 2199.
(22) Keefer, K. D.; Schaefer, D. W. *Phys. Rev. Lett.* **1986**, *56*, 2376.
(23) Kratky, O.; Porod, G. *Recl. Trav. Chim. Pays-Bas* **1949**, *68*, 1106.
(24) Kirste, R. G.; Oberthür, R. C. In *Small-angle X-ray Scattering*; Glatter, O., Kratky, O. Eds.; Academic Press: London, 1982; p 387.